QALAAI ZANISTSCIENTIFIC JOURNAL
A Scientific Quarterly Refereed Journal Issued by Lebanese French University – Erbil, Kurdistan, Iraq
Vol. (9), No (1), Spring2024
ISSN 2518-6566 (Online) - ISSN 2518-6558 (Print)

Parametric Investigations on Laminated Composite Sandwich Plates with Honeycomb Core

Master student Hozan Abdul-Jabbar Othman
Department of Mechanical and Mechatronics, College of Engineering, Salahaddin University, Erbil, Kurdistan Region, Iraq.
hozan.a.othman91@gmail.com

Dr. Shiren Othman Muhammad
Department of Mechanical and Mechatronics, College of Engineering, Salahaddin University, Erbil, Kurdistan Region, Iraq
shireen.muhammad@su.edu.krd

ARTICLE INFO

Article History:
Received: 2/1/2023
Accepted: 16/2/2023
Published: Spring2024

Keywords:
laminated composite, deflection, analytical solution, honeycomb core, Kevlar fibers, glass fibers.

Doi:
10.25212/lfu.qzj.9.1.42

ABSTRACT

In this study, an analytical solution of multi layered laminated composite laminate plate is presented of a new form of composite sandwich panels in two different styles; Kevlar fibers bonded with honeycomb core in mid plane, and glass fibers bonded with honeycomb core in mid plane. Classical laminated plate theory has been used for modeling the sandwich plate, Ritz method has been used for calculating the plate's maximum bending deflections. The results have been validated by Finite Element analysis with a good. The parametric investigations include, change in material types of lamina, different layer thicknesses, and several geometric cell shapes of honeycomb core laminated has been examined. The results proved that the Convex cell honeycomb core plays a great role in absorbing the force energy as a result it reduced the plate deflection by 8% better than semi-entrant and re-entrant, and Kevlar-49 is the best among other types of Kevlar. S_2-glass fiber -Sandwich plates have reduced the plate's overall deflections by 14.73% compared to Kevlar-29 -Sandwich plates.

QALAAI ZANISTSCIENTIFIC JOURNAL
A Scientific Quarterly Refereed Journal Issued by Lebanese French University – Erbil, Kurdistan, Iraq
Vol. (9), No (1), Spring2024
ISSN 2518-6566 (Online) - ISSN 2518-6558 (Print)

1. Introduction

Composite materials are widely utilized in the aerospace, marine, vehicle, and military armored systems sectors, among other industries (Jones, 1999, and Al Hilli, 2006). High specific strength and stiffness, exceptional formability, and corrosion resistance are just a few of the advantages of this family of materials. The laminated fiber composite is one of the most popular, with some of them passing in the higher specific moduli, such as Kevlar and carbon fiber composites. They have much higher specific strength and stiffness than monolithic materials like steel and aluminum, making them appealing for a variety of weight-sensitive applications, and one of the important applications of composite materials is body armor (Al Hilli, 2006). Body armor is a type of protective clothing that is worn to protect the human body from different types of sharp objects or projectiles. Hard body armor and soft body armor are the two types of body armor that are commonly used. Soft body armor is made up of several layers of high-performance materials, making it lighter and more flexible (Greene et al., 2018; Mukasey, Sedgwick, & Hagy, 2008). To prepare the soft body armor plates, 20–40 layers of woven or unidirectional fabrics made from high performance fibers are stitched together. Nowadays, Honeycomb composite structures are used in body armor. The sandwich panels consist of two face sheets of layered fibers, which are bonded to a very lightweight honeycomb core of aluminum. Compared to normal plates, sandwich panels have a very high stiffness and simultaneously a low weight. The core of these structures is mainly subjected to shear stresses. (Al-Mezrakchi, Al-Ramthan, & Alam, 2020) Proposed two composite plates with honeycomb core are subjected to ballistic impact. After validation of models with experimental test results, the numerical technique was successfully used to forecast impact behavior. When compared to other aluminum alloys investigated in this study, the aluminum 7039 alloy was chosen for the honeycomb core material because it had a higher ballistic resistance. After conducting tests to determine the ballistic resistance of aluminum honeycomb panels exposed to cylindrical steel impactors, (Nia, Razavi, & Majzoobi, 2008) demonstrated an analytical formulation to compute the ballistic limit velocity of metallic honeycomb structures. On the other

QALAAI ZANISTSCIENTIFIC JOURNAL
A Scientific Quarterly Refereed Journal Issued by Lebanese French University – Erbil, Kurdistan, Iraq
Vol. (9), No (1), Spring2024
ISSN 2518-6566 (Online) - ISSN 2518-6558 (Print)

hand, Different shear deformation theories for laminated plates have been developed to include the effect of transverse shear deformation. These are the classical plate theory (CPT), the first-order shear deformation theory (FSDT) and Reddy's higher-order shear deformation theory (HSDT). Fundamental governing equations for nonlinear dynamic analysis of laminated plates based on von Karman's large deflection plate theory were derived by (J. N. Reddy, 1983) and (J. Reddy & Chao, 1981). In recent years, linear and nonlinear analyses of laminated composite plate and shell structures have found increased applications (J. Reddy & Chandrashekhara, 1987) and (Baltacıoğlu, Civalek, Akgöz, & Demir, 2011). Deflection analysis of laminated plates resting on Ritz method has also been investigated by many researchers. (Nath & Shukla, 2001)and (Shukla & Nath, 2000) presented some solutions for nonlinear analysis of laminated plates. Nonlinear static and dynamic response of laminated plates are also investigated by (Nath, Prithviraju, & Mufti, 2006) and (Nath, Varma, & Mahrenholtz, 1986) using the Chebyshev series method. Rectangular plates on elastic foundation have been analyzed using analytical and numerical approaches by (Dumir & Bhaskar, 1988) and (Dumir, 1988). By using the differential quadrature and finite difference coupled approach, nonlinear static and dynamic analyses of isotropic plates and shells have been investigated by the present author (Civalek, 2005), and (Civalek, 2006). Some exact and numerical solutions of static and dynamic analyses of isotropic and laminated composite plates with or without elastic foundations are also presented in the literature (Shen, 1999), (Shen, 2000), and (Sofiyev & Schnack, 2003). In the past ten years, some new methods for numerical analysis of partial differential equations in applied mechanics have become popular (Baltacıoğlu et al., 2011). (Bhimaraddi, 1987)proposed a shear deformation theory and for static and dynamic response of the laminate and compared the results with the results obtained by Classical and Mindlin-type plate theory. Further, investigation of the dynamic response is examined by using higher-order mid-plane kinematics and concluded that the higher-order theory is more efficient to predict the responses. The principal of orthogonality and state variables are used to get the exact solution for the dynamic response of laminate via HSDT (Khdeir & Reddy, 1989). The

QALAAI ZANISTSCIENTIFIC JOURNAL
A Scientific Quarterly Refereed Journal Issued by Lebanese French University – Erbil, Kurdistan, Iraq
Vol. (9), No (1), Spring2024
ISSN 2518-6566 (Online) - ISSN 2518-6558 (Print)

analytical procedure is used to obtain the closed-form solution for the dynamic responses of the laminate with different boundary restrictions (Dewangan, Katariya, & Panda, 2020). This seeks for the high performance composite laminated plate for soft body armor. It used to calculate mid plane deflection of the rectangular composited plate due to impact velocity. The composite plate was made of Kevlar fiber renforced plate (KFRP), Glass fiber renforced plate (GFRP), and hoeycomb core. Deflection due different types of woven (KFRP), different types of woven (GFRP), several laminate thicknes of composite plate has been examined, and honeycomb core was calculated. The analytical model results were validated by ANSYS workbench.

2. Mathematical modelling

A laminated rectangular plate of dimensions a, b, and h as shown in Figure (1) is considered. A cartesian coordinate system xy is located in the middle surface of the plate.

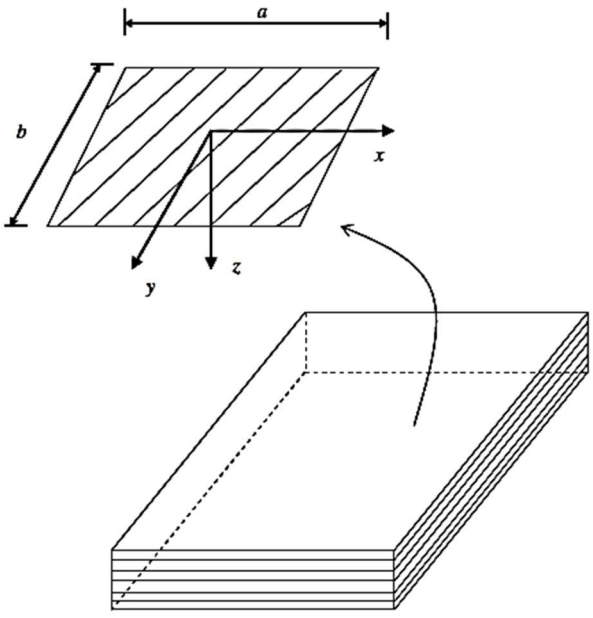

QALAAI ZANISTSCIENTIFIC JOURNAL
A Scientific Quarterly Refereed Journal Issued by Lebanese French University – Erbil, Kurdistan, Iraq
Vol. (9), No (1), Spring2024
ISSN 2518-6566 (Online) - ISSN 2518-6558 (Print)

Figure (1): Geometry and coordinate system of the laminated rectangular plate (Baltacıoğlu et al., 2011)

The displacement field at a point in the plate using the Classical Laminate Plate Theory (CLPT) of mid plane symmitric ply and angle-ply laminated plate are analyzed. Depending on the boundary conditions, the Ritz method is used. Fundamental governing equations for nonlinear dynamic analysis of laminated plates based on von Karman's large deflection plate theory were derived by (J. N. Reddy, 1983) and (J. Reddy & Chao, 1981). (J. N. Reddy, 2003) investigate governing equations in terms of the displacement. Start with linear equation of motion of the (CLPT):

$$A_{11}\frac{\partial^2 u_o}{\partial x^2}+2\,A_{16}\frac{\partial^2 u_o}{\partial x\partial y}+A_{66}\frac{\partial^2 u_o}{\partial y^2}+A_{16}\frac{\partial^2 v_o}{\partial x^2}+(A_{12}+\,A_{66})\frac{\partial^2 v_o}{\partial x\partial y}$$
$$+A_{26}\frac{\partial^2 v_o}{\partial y^2}-\left[B_{11}\frac{\partial^3 w_o}{\partial x^3}+3\,B_{16}\frac{\partial^3 w_o}{\partial x^2\partial y}+(B_{12}+\,2\,B_{66})\,\frac{\partial^3 w_o}{\partial x\partial y^2}\right. \qquad (1)$$
$$\left.+\,B_{26}\frac{\partial^3 w_o}{\partial y^3}\right]=I_o\ddot{u}_o-\,I_1\frac{\partial\ddot{w}_o}{\partial x}$$

$$A_{16}\frac{\partial^2 u_o}{\partial x^2}+(A_{12}+\,A_{66})\frac{\partial^2 u_o}{\partial x\partial y}+A_{26}\frac{\partial^2 u_o}{\partial y^2}+A_{66}\frac{\partial^2 v_o}{\partial x^2}+2\,A_{26}\frac{\partial^2 v_o}{\partial x\partial y}+A_{22}$$
$$-\left[B_{16}\frac{\partial^3 w_o}{\partial x^3}+(B_{12}+\,2\,B_{66})\,\frac{\partial^3 w_o}{\partial x^2\partial y}+3\,B_{26}\frac{\partial^3 w_o}{\partial x\partial y^2}\right. \qquad (2)$$
$$\left.+\,B_{22}\frac{\partial^3 w_o}{\partial y^3}\right]=\,I_o\ddot{v}_o-\,I_1\frac{\partial\ddot{w}_o}{\partial y}$$

QALAAI ZANISTSCIENTIFIC JOURNAL
A Scientific Quarterly Refereed Journal Issued by Lebanese French University – Erbil, Kurdistan, Iraq
Vol. (9), No (1), Spring2024
ISSN 2518-6566 (Online) - ISSN 2518-6558 (Print)

$$
\begin{aligned}
&B_{11}\frac{\partial^3 u_o}{\partial x^3} + 3\,B_{16}\frac{\partial^3 u_o}{\partial x^2 \partial y} + (B_{12} + 2\,B_{66})\,\frac{\partial^3 u_o}{\partial x \partial y^2} + B_{26}\frac{\partial^3 u_o}{\partial y^3} + B_{16}\frac{\partial^3 v_o}{\partial x^3} \\
&\quad + (B_{12} + 2\,B_{66})\,\frac{\partial^3 v_o}{\partial x^2 \partial y} + 3\,B_{26}\frac{\partial^3 v_o}{\partial x \partial y^2} + B_{22}\frac{\partial^3 v_o}{\partial y^3} \\
&\quad - \left[D_{11}\frac{\partial^4 w_o}{\partial x^4} + 4\,D_{16}\frac{\partial^4 w_o}{\partial x^3 \partial y} + 2\,(D_{12} + 2\,D_{66})\,\frac{\partial^4 w_o}{\partial x^2 \partial y^2}\right. \\
&\quad \left. + 4\,D_{26}\frac{\partial^4 w_o}{\partial x \partial y^3} + D_{22}\frac{\partial^4 w_o}{\partial y^4}\right] + \hat{N}_{xx}\frac{\partial^2 w_o}{\partial x^2} + 2\,\hat{N}_{xy}\frac{\partial^2 w_o}{\partial x \partial y} \\
&\quad + \hat{N}_{yy}\frac{\partial^2 w_o}{\partial y^2} + q \\
&\quad = I_1\left(\frac{\partial \ddot{u}_o}{\partial x} + \frac{\partial \ddot{u}_o}{\partial y}\right) + I_o \ddot{w}_o - I_2\left(\frac{\partial^2 \ddot{w}_o}{\partial x^2} + \frac{\partial^2 \ddot{w}_o}{\partial y^2}\right)
\end{aligned}
\tag{3}
$$

where $\hat{N}_{xx}$, $\hat{N}_{xy}$, and $\hat{N}_{yy}$ are the applied edge forces.

Eqs (1, 2, 3) in the differential operator form are

$$
\begin{bmatrix} c_{11} & c_{12} & c_{13} \\ c_{12} & c_{22} & c_{23} \\ c_{13} & c_{23} & c_{33} \end{bmatrix}\begin{bmatrix} u_0 \\ v_0 \\ w_0 \end{bmatrix} + \begin{bmatrix} m_{11} & 0 & m_{13} \\ 0 & m_{22} & m_{23} \\ m_{13} & m_{23} & m_{33} \end{bmatrix}\begin{bmatrix} \ddot{u}_o \\ \ddot{v}_o \\ \ddot{w}_o \end{bmatrix} = \begin{bmatrix} 0 \\ 0 \\ \mathrm{q} \end{bmatrix} \tag{4}
$$

Where c_{ij} cofficients are defined as

$$
\begin{aligned}
c_{11} &= A_{11}\,dx^2 + 2\,A_{16}\,dx\,dy + A_{66}\,dy^2 \\
c_{12} &= A_{16}\,dx^2 + (A_{12} + A_{66})\,dx\,dy + A_{66}\,dy^2 \\
c_{13} &= -\left[B_{11}\,dx^3 + 3\,B_{16}\,dx^2\,dy + (B_{12} + 2\,B_{66})\,dx\,dy^2 + B_{26}\,dy^3\right] \\
c_{22} &= A_{22}\,dx^2 + 2\,A_{26}\,dx\,dy + A_{22}\,dy^2 \\
c_{23} &= -\left[B_{16}\,dx^3 + (B_{12} + 2\,B_{66})\,dx^2\,dy + 3\,B_{26}\,dx\,dy^2 + B_{22}\,dy^3\right] \\
c_{33} &= D_{11}\,dx^4 + 4\,D_{16}\,dx^3\,dy + 2\,(D_{12} + 2\,D_{66})dx^2\,dy^2 \\
&\quad + 4D_{26}\,dx\,dy^3 + D_{66}\,dy^4 \\
&\quad - \left[\hat{N}_{xx}\,dx^2 + 2\,\hat{N}_{xy}\,dx\,dy + \hat{N}_{yy}\,dy^2\right]
\end{aligned}
\tag{5}
$$

QALAAI ZANISTSCIENTIFIC JOURNAL
A Scientific Quarterly Refereed Journal Issued by Lebanese French University – Erbil, Kurdistan, Iraq
Vol. (9), No (1), Spring2024
ISSN 2518-6566 (Online) - ISSN 2518-6558 (Print)

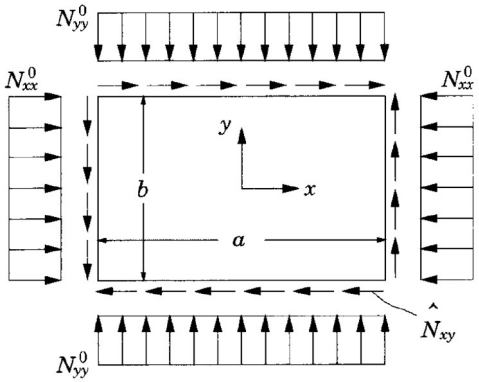

Figure (2): Rectangular plate with in-plane compressive edge forces (J. N. Reddy, 2003) $(\widehat{N}_{xx} = -N_{xx}^o\ ,\ \widehat{N}_{yy} = -N_{yy}^o)$.

m_{ij} cofficients are defined as

$$m_{11} = -I_o\,dt^2 \quad , \quad m_{13} = I_1\,dx\,dt^2 \quad , \quad m_{22} = -I_o\,dt^2$$
$$m_{23} = I_1\,dy\,dt^2 \quad , \quad m_{33} = I_o\,dt^2\,(dx^2 + dy^2) \tag{6}$$

And d_t^i denote the differenitial operators

$$d_t^i = \frac{\partial^i}{\partial x^i} \quad , \quad d_t^i = \frac{\partial^i}{\partial y^i} \quad , \quad d_t^i = \frac{\partial^i}{\partial t^i} \quad , \quad \text{for} \quad (i = 1,2,3,4) \tag{7}$$

where (A_{ij} , B_{ij} , D_{ij}) are called (extensional, coupling, and bending) stiffnesses, which defined in the term of lamina stiffnesses $\left[(\bar{Q}_{ij})\right]_k$ as

$$A_{ij} = \sum_{k=1}^{n}\left[(\bar{Q}_{ij})\right]_k (h_k - h_{k-1}) \quad , \quad B_{ij} = \frac{1}{2}\sum_{k=1}^{n}\left[(\bar{Q}_{ij})\right]_k (h_k^2 - h_{k-1}^2)$$
$$D_{ij} = \frac{1}{3}\sum_{k=1}^{n}\left[(\bar{Q}_{ij})\right]_k (h_k^3 - h_{k-1}^3) \tag{8}$$

$$\bar{Q}_{11} = Q_{11}c^4 + Q_{22}s^4 + 2(Q_{12} + 2Q_{66})c^2s^2$$
$$\bar{Q}_{12} = (Q_{11} + Q_{22} - 4Q_{66})c^2s^2 + Q_{12}(c^4 + s^4) \tag{9}$$
$$\bar{Q}_{22} = Q_{11}s^4 + Q_{22}c^4 + 2(Q_{12} + 2Q_{66})c^2s^2$$

QALAAI ZANISTSCIENTIFIC JOURNAL
A Scientific Quarterly Refereed Journal Issued by Lebanese French University – Erbil, Kurdistan, Iraq
Vol. (9), No (1), Spring2024
ISSN 2518-6566 (Online) - ISSN 2518-6558 (Print)

$$\bar{Q}_{16} = (Q_{11} - Q_{12} - 2Q_{66})c^3 s - (Q_{22} - Q_{12} - 2Q_{66})cs^3$$
$$\bar{Q}_{26} = (Q_{11} - Q_{12} - 2Q_{66})s^3 c - (Q_{22} - Q_{12} - 2Q_{66})sc^3$$
$$\bar{Q}_{66} = (Q_{11} + Q_{22} - 2Q_{12} - 2Q_{66})s^2 c^2 + Q_{66}(s^4 + c^4)$$

2.1 Ritz method

The Navier and levy type solutions do not exist for rectangular plates with all four sides clamped. Therefore, for this case the approximate solution method was used to solve this problem. Let us consider Ritz method to determine the bending deflection for especially orthotropic rectangular plate with clamped edge (J. N. Reddy, 2003). Ritz method has been considered for the determination of bending deflections for any points are:

- The plate is symmetric about mid-plane, and each ply has the same thickness (the composite plate consists of Kevlar layers and glass layers that consist of the same laminate thickness with honeycomb), hence all the bending extension coupling stiffness B_{ij} are zero.
- The effect of vibration on the composite plate was neglected, then $(I_o,\ I_1,\ I_2)$ are zero.
- The plate consists of especially orthotropic laminates, the layer stiffnesses $\bar{Q}_{16}, \bar{Q}_{26}, \text{and } \bar{Q}_{45}$ are zero for cross-ply angles (0/90), then $A_{16}, A_{26}, D_{16}, D_{26}$, and A_{26} are zero.
- $(D_{11} = D_{22}\ , \text{and } D_{12} = D_{21})$, Because of each ply consists of woven fibers by (0/90) plies fixed together as one ply $(E_1 = E_2)$ was used in this study.

The Ritz solutions can be developed for rectangular laminates with all four edges are clamped boundary conditions. The boundary conditions for a rectangular plate that clamped all four edges used in the analytical solution are:

$$\text{at } x = 0, a \qquad w_o = 0 \text{ and } \frac{\partial w_o}{\partial x} = 0 \tag{10}$$

QALAAI ZANISTSCIENTIFIC JOURNAL
A Scientific Quarterly Refereed Journal Issued by Lebanese French University – Erbil, Kurdistan, Iraq
Vol. (9), No (1), Spring2024
ISSN 2518-6566 (Online) - ISSN 2518-6558 (Print)

$$\text{at } y = 0, b \quad w_o = 0 \text{ and } \frac{\partial w_o}{\partial y} = 0$$

The boundary conditions in Eq. (10) imply the following CCCC boundary conditions on the displacements and stress resultants of the classical laminate theory (J.N. REDDY, 2004). Another assumption the applied force only acting on Z direction with neglecting the vibration of the plate Eq (3) becomes:

$$\begin{aligned} 0 = \iint_A \Bigg[& D_{11}\left(\frac{\partial^2 w_o}{\partial x^2}\frac{\partial^2 w_o}{\partial x^2}\right) \\ & + 2D_{12}\left(\frac{\partial^2 w_o}{\partial x^2}\frac{\partial^2 w_o}{\partial y^2} + \frac{\partial^2 w_o}{\partial x^2}\frac{\partial^2 w_o}{\partial y^2}\right) \\ & + D_{22}\left(\frac{\partial^2 w_o}{\partial y^2}\frac{\partial^2 w_o}{\partial y^2}\right) + 4D_{66}\left(\frac{\partial^2 w_o}{\partial x \partial y}\frac{\partial^2 w_o}{\partial x \partial y}\right) \\ & - q\delta w_o \Bigg] \end{aligned} \tag{11}$$

$$\begin{aligned} \mathrm{II} w_o = \frac{1}{2}\iint_A \Bigg[& D_{11}\left(\frac{\partial^2 w_o}{\partial x^2}\right) + 2D_{12}\frac{\partial^2 w_o}{\partial x^2}\frac{\partial^2 w_o}{\partial y^2} + D_{22}\left(\frac{\partial^2 w_o}{\partial y^2}\right)^2 \\ & + 4D_{66}\left(\frac{\partial^2 w_o}{\partial x \partial y}\right)^2 - 2qw_o \Bigg] dxdy \end{aligned} \tag{12}$$

This expression should be appended with appropriate terms due to any applied edge moments and forces.

2.2 Determination equations of bending deflection:

Consider a rectangular plate with all four edges clamped and subjected to distributed transvers load q(x, y). The boundary condition for clamped composite plate are shown in Figure (3)

QALAAI ZANISTSCIENTIFIC JOURNAL
A Scientific Quarterly Refereed Journal Issued by Lebanese French University – Erbil, Kurdistan, Iraq
Vol. (9), No (1), Spring2024
ISSN 2518-6566 (Online) - ISSN 2518-6558 (Print)

$$\text{at } x = 0 \text{ and } x = a \ , \quad w_o = 0 \ , \text{and} \quad \frac{\partial w_o}{\partial x} = 0$$

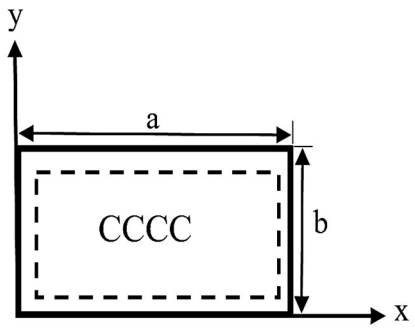

$$\text{at } y = 0, \text{ and } y = b \ , \quad w_o = 0 \ , \text{and} \quad \frac{\partial w_o}{\partial y} = 0$$

Figure (3): Four edge clamped boundary conditions for composite plate

According to the assumption of Ritz approximation method for all four-edge clamped in the form:

$$w_o(x,y) \approx Wmn(x,y) = \sum_i^m \sum_j^n c_{ij}\, \varphi_{ij}(x,y) \tag{13}$$

where φ_{ij} is the approximation functions that satisfy all the geometric boundary, for this problem, both Ritz and Galerkin give the same solution for the same kind of approximation functions.

For the rectangular plate at clamped boundary condition, the approximation function $\varphi_{ij}\ (x,y)$ is

$$\varphi_{ij}\ (x,y) = X_i(x) Y_j(y) \tag{14}$$

where

$$X_i(x) = \left(\frac{x}{a}\right)^{i+1} \left(1 - \frac{x}{a}\right)^2 \tag{15}$$

QALAAI ZANISTSCIENTIFIC JOURNAL
A Scientific Quarterly Refereed Journal Issued by Lebanese French University – Erbil, Kurdistan, Iraq
Vol. (9), No (1), Spring2024
ISSN 2518-6566 (Online) - ISSN 2518-6558 (Print)

$$Y_j(y) = \left(\frac{y}{b}\right)^{j+1}\left(1-\frac{y}{b}\right)^2$$

or

$$\begin{aligned} X_i(x) &= \sin\lambda_i x - \sinh\lambda_i x + \alpha_i(\cos\lambda_i x - \cosh\lambda_i x) \\ Y_j(y) &= \sin\lambda_j y - \sinh\lambda_j y + \alpha_j(\cosh\lambda_j y - \cos\lambda_j y) \end{aligned} \tag{16}$$

for *i*= 1,2,3,….,m; and *j*=1,2,3,….,n.

where

and $$\cos\lambda_i a\cosh\lambda_i a - 1 = 0 \tag{17}$$

$$\alpha_i = \frac{\sin\lambda_i a - \sinh\lambda_i a}{\cosh\lambda_i a - \cos\lambda_i a} = \frac{\cosh\lambda_i a - \cos\lambda_i a}{\sin\lambda_i a - \sinh\lambda_i a} \tag{18}$$

By substituting Eq. (13) , and given φ_{ij} by Eq. (14)

$$\delta w_o = \sum_p^m \sum_q^n \delta c_{pq}\varphi_{pq} \tag{19}$$

Then applying to Eq. (10), obtain

$$\begin{aligned} 0 = \sum_p^m \sum_q^n \Bigg\{ \sum_i^m \sum_j^n c_{ij} \int_0^b \int_0^a \Bigg[& D_{11}\frac{d^2X_i}{dx^2}Y_j\frac{d^2X_p}{dx^2}Y_q + 4D_{66}\frac{dX_i}{dx}\frac{dY_j}{dy}\frac{dX_p}{dx}\frac{dY_q}{dy} \\ & + D_{12}\left(X_i\frac{d^2Y_j}{dy^2}\frac{d^2X_p}{dx^2}Y_q + \frac{d^2X_i}{dx^2}Y_jX_p\frac{d^2Y_q}{dy^2}\right) \\ & + D_{22}X_i\frac{d^2Y_j}{dy^2}X_p\frac{d^2Y_q}{dy^2}\Bigg] dxdy - \int_0^b\int_0^a qX_pY_q dxdy \Bigg\}\delta c_{pq} \end{aligned} \tag{20}$$

QALAAI ZANISTSCIENTIFIC JOURNAL
A Scientific Quarterly Refereed Journal Issued by Lebanese French University – Erbil, Kurdistan, Iraq
Vol. (9), No (1), Spring2024
ISSN 2518-6566 (Online) - ISSN 2518-6558 (Print)

$$0=\left\{\sum_{i}^{m}\sum_{j}^{n}\int_{0}^{b}\int_{0}^{a}\left[D_{11}\frac{d^2X_i}{dx^2}Y_j\frac{d^2X_p}{dx^2}Y_q+4D_{66}\frac{dX_i}{dx}\frac{dY_j}{dy}\frac{dX_p}{dx}\frac{dY_q}{dy}\right.\right.$$
$$+D_{12}\left(X_i\frac{d^2Y_j}{dy^2}\frac{d^2X_p}{dx^2}Y_q+\frac{d^2X_i}{dx^2}Y_jX_p\frac{d^2Y_q}{dy^2}\right) \quad (21)$$
$$\left.\left.+D_{22}X_i\frac{d^2Y_j}{dy^2}X_p\frac{d^2Y_q}{dy^2}\right]dxdy\right\}c_{ij}-\int_{0}^{b}\int_{0}^{a}qX_pY_qdxdy$$

Eq. (21) represents $m\times n$ algebraic equations among the coefficients c_{ij}, and all integral are line integrals, and they involve evaluating five different integrals

$$\int_0^a X_i\,dx,\int_0^a X_i\;X_p\,dx,\quad\int_0^a\frac{dX_i}{dx}\frac{dX_p}{dx}dx$$
$$\int_0^a X_i\;\frac{d^2X_p}{dx^2}dx,\quad\int_0^a\frac{d^2X_i}{dx^2}\frac{d^2X_p}{dx^2}dx, \quad (22)$$

Consider the algebraic functions with *m=n=1* and $q=q_o$. The integrals in Eq. (22) for this case given by

$$\int_0^a X_i\,dx=\frac{a}{30},\int_0^a X_1\;X_1\,dx=\frac{a}{630},\quad\int_0^a\frac{dX_1}{dx}\frac{dX_1}{dx}dx=\frac{2}{105a}$$
$$\int_0^a X_1\;\frac{d^2X_1}{dx^2}dx=-\frac{2}{105a},\quad\int_0^a\frac{d^2X_1}{dx^2}\frac{d^2X_1}{dx^2}dx=\frac{4}{5a^3} \quad (23)$$

Substituting the integral values into Eq. (21), and obtain

$$0=\left[\left(\frac{b}{630}\right)\left(\frac{4}{5a^3}\right)D_{11}+4D_{66}\left(\frac{2}{105a}\right)\left(\frac{2}{105b}\right)+2D_{12}\left(-\frac{2}{105a}\right)\left(-\frac{2}{105b}\right)\right.$$
$$\left.+\left(\frac{a}{630}\right)\left(\frac{4}{5b^3}\right)D_{22}\right]c_{11}-\left(\frac{a}{30}\right)\left(\frac{b}{30}\right)q_o \quad (24)$$

or

QALAAI ZANISTSCIENTIFIC JOURNAL
A Scientific Quarterly Refereed Journal Issued by Lebanese French University – Erbil, Kurdistan, Iraq
Vol. (9), No (1), Spring2024
ISSN 2518-6566 (Online) - ISSN 2518-6558 (Print)

$$\left[\frac{7}{a^4}D_{11}+\frac{4}{a^2b^2}(D_{12}+2D_{66})+\frac{7}{b^4}D_{22}+\right]c_{11}=\frac{49}{8}q_o \quad (25)$$

and one parameter solution becomes

$$W_{11}(x,y)=\left(\frac{49}{8}\right)\frac{q_o a^4\left[\frac{x}{a}-\left(\frac{x}{a}\right)^2\right]^2\left[\frac{y}{b}-\left(\frac{y}{b}\right)^2\right]^2}{7D_{11}+4(D_{12}+2D_{66})s^2+7D_{22}s^4} \quad (26)$$

where s=a/b denotes the plate aspect ratio. The maximum deflection occurs at x=a/2 and y=b/2:

$$W_{11}(\frac{a}{2},\frac{b}{2})=0.00342\frac{q_o a^4}{D_{11}+0.5714(D_{12}+2D_{66})s^2+D_{22}s^4} \quad (27)$$

For isotropic square plate $(\mathrm{a/b}=1, D_{11}=D_{22}=D_{12}+2D_{66}=D)$, the maximum central deflection becomes

$$W_{11}(\frac{a}{2},\frac{b}{2})=0.00126\frac{q_o a^4}{D} \quad (28)$$

where W_{11} is the central deflection along the z direction, a, and b are length and width of the composite plate according x, and y direction, respectively, $\boldsymbol{q_o}$ is the intensity of transverse distributed load per unit area of the composite plate, D is the bending stiffness of composite plate.

3. Parametric investigations

3.1 Material investigation

This study uses two types of sandwich plate: aluminum honeycomb core with Kevlar fibers and Glass fiber as face sheet. Different types of Glass fiber (E-glass, C-glass, R-glass, S2-glass, AR-glass, D-glass, A-glass, and EGR-glass) whereas Table (1) lists their intrinsic characteristics, and different types of Kevlar fibers (Kevlar 29, Kevlar49, and Kevlar 149) are used, and Table (2) lists their mechanical characteristics. The mechanical properties like modulus of elasticity (E), passion's ratio (v), and shear

QALAAI ZANISTSCIENTIFIC JOURNAL
A Scientific Quarterly Refereed Journal Issued by Lebanese French University – Erbil, Kurdistan, Iraq
Vol. (9), No (1), Spring2024
ISSN 2518-6566 (Online) - ISSN 2518-6558 (Print)

modulus (G) used as fiber without epoxy, in this study assumed as woven fiber ($E_1=E_2$).

Table (1): Properties of different types of glass fibers (Kaw,2005, and Reddy, 2003).

No.	Glass fiber	density(g/cm^3)	Tensile strength(GPa)	young's modulus(GPa)
1	E-glass	2.58	3.445	72.3
2	c-glass	2.52	3.31	68.9
3	S2-glass	2.46	4.89	86.9
4	A-glass	2.44	3.31	68.9
5	D-glass	2.11	2.415	51.7
6	R-glass	2.54	4.135	85.5
7	EGR-glass	2.72	3.445	80.3
8	AR-glass	2.7	3.241	73.1

Table (2): Properties of different types of glass fiber (Kaw, 2005).

No.	Kevlar fiber	density(g/cm^3)	Tensile strength(GPa)	Young's modulus(GPa)
1	Kevlar 29	1.44	2.9	62.05
2	Kevlar 49	1.48	2.9	131
3	Kevlar 149	1.47	2.3	143

3.2 Layer thickness investigation

Three different groups of layer thicknesses are used in this study; first different layer thickness (0.2, 0.3, 0.4, 0.5, 0.6) mm used for each ply of glass fibers with constant Aluminum honeycomb core 20 mm; second changed layer thickness of Kevlar by (0.1, 0.2, 0.3, 0.4, 0.5) mm used for each ply of Kevlar fibers with 20mm of Aluminum honeycomb core; and finally different Aluminum honeycomb core thickness (10, 14, 20) mm with 0.3 mm layer thickness of each ply of Kevlar, and glass fiber.

3.3 Geometrical investigation

Cross woven fiber 0/90(E1=E2) ply of Kevlar, and glass fibers used with constant layer thickness 0.3 mm to each layer with three types of cell shape of aluminum honeycomb core (Convex, semi-entrant, re-entrant) as shown in Figure (4).

QALAAI ZANISTSCIENTIFIC JOURNAL
A Scientific Quarterly Refereed Journal Issued by Lebanese French University – Erbil, Kurdistan, Iraq
Vol. (9), No (1), Spring2024
ISSN 2518-6566 (Online) - ISSN 2518-6558 (Print)

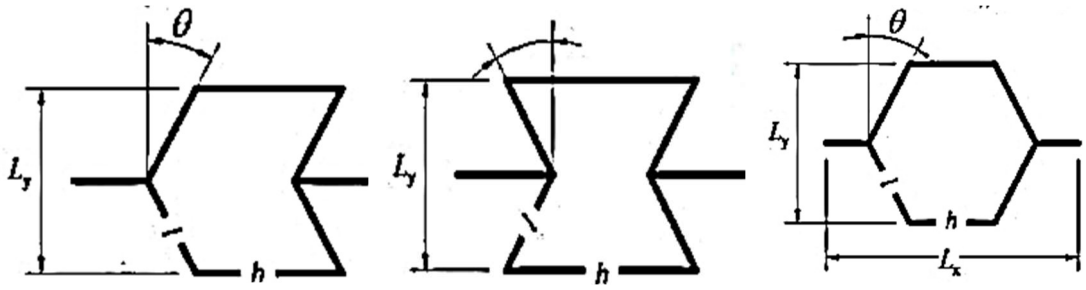

(a) (b) (c)

Figure (4): Geometrics of honeycomb cores with different cell shapes (a): semi-re-entrnt, (b): re-entrnt, and (c): convex (Luo, Yuan, Shen, & Liu, 2021).

The linear elastic response of honeycomb core is preliminary caused by bending of the cell walls. (Gibson, Ashby, Schajer, & Robertson, 1982) modeled each wall as a beam. The geometrical hexagonal cell as showed in Figure (5).

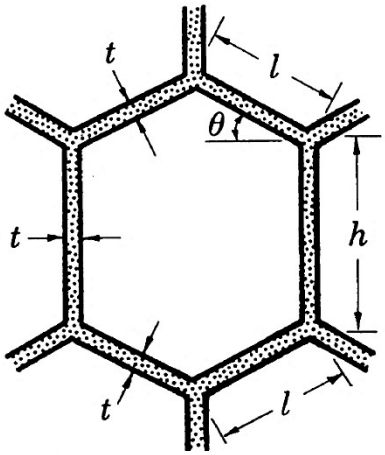

Figure (5): Geometry of hexagonal cell of honeycomb core (Gibson et al., 1982).

$$E_1 = E_a \frac{t^3}{l^3} \frac{\cos\theta}{(h/l + \sin\theta)\sin^2\theta}. \quad (29)$$

$$E_2 = E_a \frac{t^3}{l^3} \frac{(h/l + \sin\theta)}{\cos^3\theta}. \quad (30)$$

QALAAI ZANISTSCIENTIFIC JOURNAL
A Scientific Quarterly Refereed Journal Issued by Lebanese French University – Erbil, Kurdistan, Iraq
Vol. (9), No (1), Spring2024
ISSN 2518-6566 (Online) - ISSN 2518-6558 (Print)

$$v_1 = -\frac{\varepsilon_2}{\varepsilon_1} = \frac{\cos^2\theta}{(h/l + \sin\theta)\sin\theta}. \quad (31)$$

$$v_2 = -\frac{\varepsilon_1}{\varepsilon_2} = \frac{(h/l + \sin\theta)\sin\theta}{\cos^2\theta}. \quad (32)$$

$$G = E_a \frac{t^3}{l^3} \frac{(h/l + \sin\theta)}{(h/l)^2(2\,h/l + 1)\cos\theta}. \quad (33)$$

where

E_a: is the modulus elasticity for aluminum.

t: is the wall thickness of aluminum honeycomb.

l, h: are the length and height of the aluminum honeycomb respectively.

θ: is cell wall angle, for regular hexagons ($\theta = 30^o$).

4. Validation

A Finite Element model was developed to predict the mechanical performance of the sandwich by using ANSYS 2021 R21 commercial program. The geometries of sandwich panel with different face-sheet thickness were modeled, and solving the finite element was produced by ANSYS/LS-DYN solver from ANSYS software. Four edge clamped plate 2288 nodes, and 1050 elements were used to simulate the skins, and 2288 nodes, and 1575 elements were used to simulate the core, as the upper and lower Kevlar-29 fiber were divided into 1144 nodes, and 525 elements, respectively. At the same time 2288 nodes, and 1575 elements utilized for modeling the honeycomb aluminum honeycomb core. Each material had a lamina property with a longitudinal elastic modulus of direction (E_x), a transverse elastic modulus (E_y), an elastic modulus in the depth direction (E_z), shear modulus of rigidity (G_{xz}, G_{yz}, G_{xy}), and Poisson ratio (v_{xy}, v_{yz}, v_{zx}). The applied load was imposed in the center of the composite plate, bending in accordance with the analytical solution. The solution was obtained through a series of load increments. Then the simulated results were compared with the theoretical values. Figure (6) shows the finite element model of

QALAAI ZANISTSCIENTIFIC JOURNAL
A Scientific Quarterly Refereed Journal Issued by Lebanese French University – Erbil, Kurdistan, Iraq
Vol. (9), No (1), Spring2024
ISSN 2518-6566 (Online) - ISSN 2518-6558 (Print)

the Kevlar-29 fibers as face-sheet, and Aluminum 5052 honeycomb core sandwich panel.

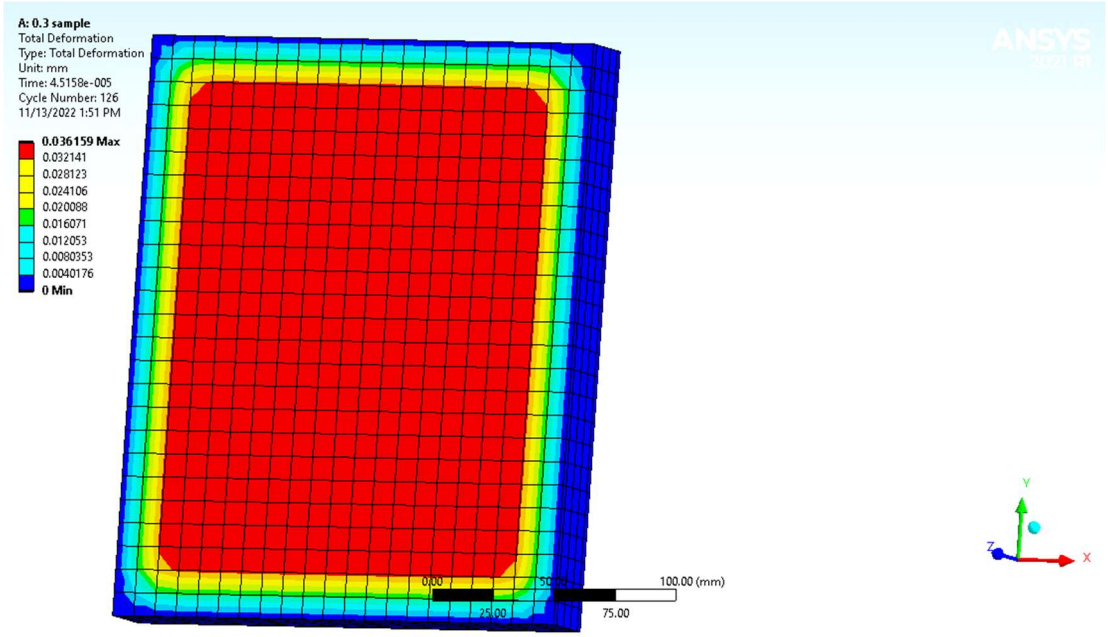

Figure (6): Finite Element simulation for Kevlar-29 face-sheet with aluminum 5052 honeycomb core, and effect of force on deflection of the composite laminated plate.

Based on Table (3), the FE and analytical solution results showed good agreement. Results showed a small difference between Finite Element and analytical simulation, because of design of the specimen and time duration in the FE model.

Table (3): Comparison of the central deflection in (m) between analytical solutions, and Finite Element (ANSYS 2021 R1 workbench) results for four ended clamped sandwich composite plate.

No.	Central deflection *W* (m) Simulation by FE	Central deflection *W* (m) Analytical solution	Percentage (%) variation between results
1	$9.3055*10^{-7}$	$9.09107*10^{-7}$	2.304

QALAAI ZANISTSCIENTIFIC JOURNAL
A Scientific Quarterly Refereed Journal Issued by Lebanese French University – Erbil, Kurdistan, Iraq
Vol. (9), No (1), Spring2024
ISSN 2518-6566 (Online) - ISSN 2518-6558 (Print)

2	$1.8611*10^{-6}$	$1.81821*10^{-6}$	2.304
3	$3.722*10^{-6}$	$3.63643*10^{-6}$	2.299
4	$4.6528*10^{-6}$	$4.54554*10^{-6}$	2.305
5	$5.5834*10^{-6}$	$5.45464*10^{-6}$	2.306
6	$6.514*10^{-6}$	$6.36375*10^{-6}$	2.307
7	$7.4445*10^{-6}$	$7.27286*10^{-6}$	2.306
8	$9.3057*10^{-6}$	$9.09107*10^{-6}$	2.306

These results suggest that the FE model could be used as a design approach to evaluate the bending performance of sandwich panels. Under the same loads, using specimen Kevlar-29 face-sheet with Aluminum 5052 honeycomb core as examples to verify the precision of the transformed section method, the elastic stage of the specimen was investigated. A comparison of the theoretical, and simulated values of the central displacement is shown in Figure (7). The comparisons of numerical and analysis results to the analytical solution, data show that the method is rather precise and is a useful auxiliary means for research work, design, and test.

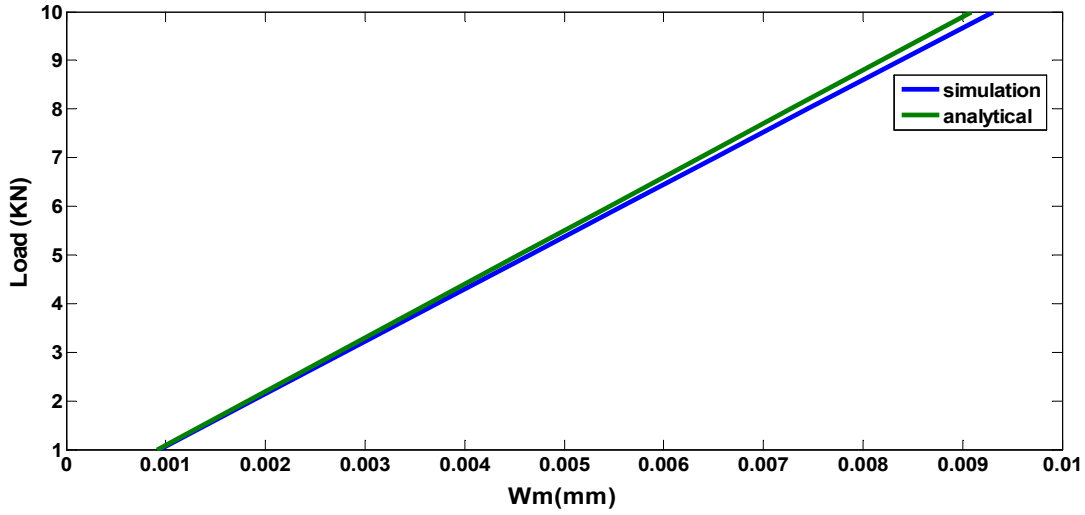

QALAAI ZANISTSCIENTIFIC JOURNAL
A Scientific Quarterly Refereed Journal Issued by Lebanese French University – Erbil, Kurdistan, Iraq
Vol. (9), No (1), Spring2024
ISSN 2518-6566 (Online) - ISSN 2518-6558 (Print)

Figure (7): Comparison of the central deflection in (mm) between analytical solutions, and Finite Element (ANSYS 2021 R1) results for four end clamped composite plate.

5. Result and discussion

Nowadays, composite plate is widely used. In this study composite sandwich plate with honeycomb core was investigated. In Figure (8) the deflection of symmetric sandwich composite plate with honeycomb core at four edges clamped boundary conditions in different face-sheet layer thickness was used, results show that the central deflection decreased as increase layer thickness or increase number of layers. When the load remained constant in small layer thicknesses the central deflection increased rapidly, but in larger layer thicknesses the central deflection increased slowly. The central deflection results agree with (Ahmed, Agarwal, Pal, & Srivastav, 2013). In this study 0.3mm thickness for each layer has been selected, as this is a suitable thickness for body armor applications. Figure (9) show the effect of load on the central deflection of composite plate made of different types of glass fiber with aluminum 5052 honeycomb core, results showed that S2-glass fiber is the best type to resist deflection and absorb more energy than other types, for this purpose Figure (10), and Figure (11) showed more details to display the best type. The effect of load on the deflection of different types of glass fiber with Aluminum 5052 honeycomb core sandwich plate for 20 layers of 0.3 mm glass fiber for each layer and 20 mm of Aluminum 5052 honeycomb core in Figure (10) compared four types (R-glass, AR-glass, A- glass, D- glass) results showed that R-glass fiber absorbed more energy than (AR-type, A-type, D-type) by 13.5%, 18%, 36.8%, respectively, and in Figure (11) compared the other four types (C- glass, E- glass, EGR- glass, S2- glass). The overall results showed that S2-glass is the best type to absorb energy, better than (R-glass, EGR- glass, AR-glass, E- glass, A- glass, C- glass, D- glass) by (1.5%, 7%, 14.8%, 16.2%, 19.3%, 20%, 37.7%) respectively, and has the minimum deflection, but D-glass has the lowest grade in energy absorption, and has the maximum deflection. Kevlar is another type of fibers that stronger than glass fiber, absorb more energy, and has minimum deflection. In Figure (12) effect of load on central deflection for different types of

QALAAI ZANISTSCIENTIFIC JOURNAL
A Scientific Quarterly Refereed Journal Issued by Lebanese French University – Erbil, Kurdistan, Iraq
Vol. (9), No (1), Spring2024
ISSN 2518-6566 (Online) - ISSN 2518-6558 (Print)

(Kevlar-29, Kevlar-49, and Kevlar-149) with aluminum 5052 honeycomb core sandwich plate. The composite plate made of 20 layers of 0.3 mm layer thickness of Kevlar with 20 mm of aluminum 5052 honeycomb core in the mid-plate, results show as the load increased to Kevlar-49, and Kevlar-149 the central deflection increased regularly without any significant phenomena, Kevlar-49 is better to absorb more energy than Kevla-149, and Kevlar-29, but Kevlar-149 has a small deference between results as compared with Kevlar-49, and for Kevlar-29 as the load increases, the deflection quickly increased due to lower contact stiffness causes lower modulus of elasticity compared with Kevlar-49 and Kevlar-149 (Al Hilli, 2006).

Another parameter effect on the performance of composite plate is layer thickness. Because of some materials produced for a special application, they are difficult to receive, in this study several layer thicknesses were examined for E-glass, and Kevlar-29 because they are easy to receive for experimental test. The effect of load-central deflection for different layer thicknesses for 20 layers of E-glass fiber, and Kevlar-29, respectively with 20 mm of aluminum 5052 honeycomb core in mid-plane. Five different layer thicknesses (0.2, 0.3, 0.4, 0.5, 0.6) mm for each ply of E-glass fiber, and (0.1, 0.2, 0.3, 0.4, 0.5) mm for Kevlar-29 was considered in Figure (13), and Figure (14), results exhibited good agreement with (Fang, Shi, Wang, Qi, & Liu, 2016), results showed in small thicknesses, as the load increases, the deflection increased quickly, but when increase layer thicknesses, as the load increases, the deflection increased slowly. As to aluminum honeycomb core different types of aluminum did not show significant difference, but effect of thickness of core, and cell shapes showed in Figure (15), and Figure (16). In Figure (15) three different thickness of aluminum 5052 honeycomb core (10, 14, and 20) mm was considered, results showed by increasing honeycomb core thickness from 10 mm to 20 mm, the energy absorption increased by 70%. In Figure (16) three types of cell shape (Convex, semi-entrant, re-entrant) was considered, and showed Convex is more effective type, absorb more energy, and made a minimum load-deflection. Figure (17) showed the effect of load on central deflection by increasing Kevlar-49 layers in (Kevlar, Glass fiber, and aluminum5052 honeycomb core) sample; due to high strength and modulus of elasticity of Kevlar-49

QALAAI ZANISTSCIENTIFIC JOURNAL
A Scientific Quarterly Refereed Journal Issued by Lebanese French University – Erbil, Kurdistan, Iraq
Vol. (9), No (1), Spring2024
ISSN 2518-6566 (Online) - ISSN 2518-6558 (Print)

layers the central deflection decreased by increasing Kevlar-49 layers instead of S_2 glass fiber.

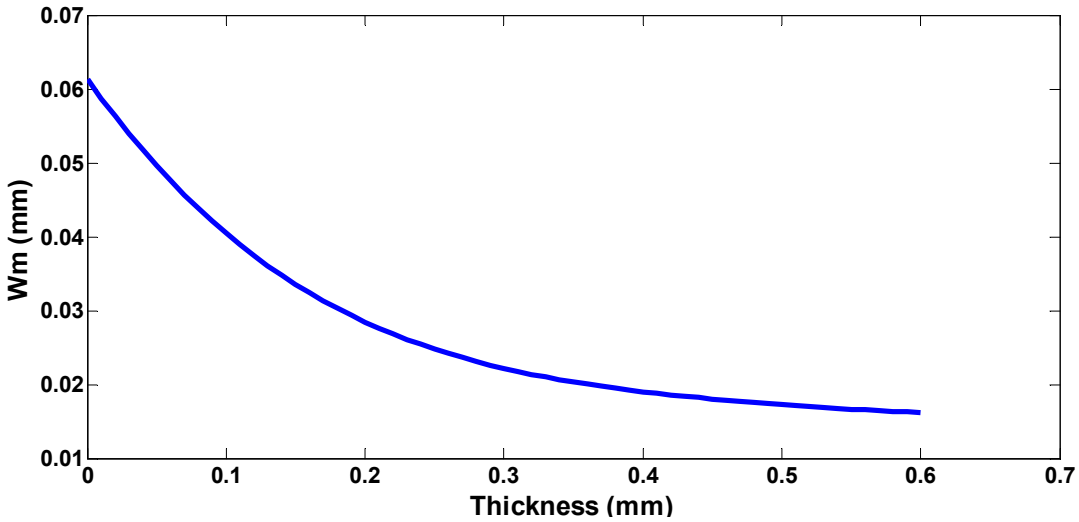

Figure (8): The deflection of symmetric sandwich composite plate with honeycomb core at four ended clamped boundary conditions in different face-sheet layer thickness.

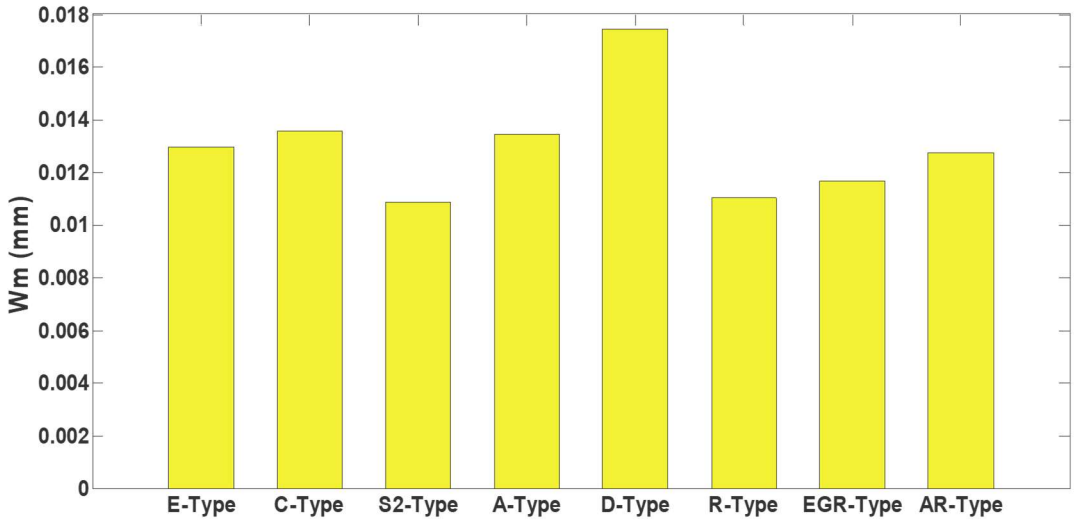

QALAAI ZANISTSCIENTIFIC JOURNAL
A Scientific Quarterly Refereed Journal Issued by Lebanese French University – Erbil, Kurdistan, Iraq
Vol. (9), No (1), Spring2024
ISSN 2518-6566 (Online) - ISSN 2518-6558 (Print)

Figure (9): Effect of different types of glass fiber on central deflection for 0.3 mm thickness for each layer of (R-glass, AR-glass, A-glass, D-glass, C-glass, E-glass, EGR-glass, and S2) with Aluminum 5052 honeycomb core.

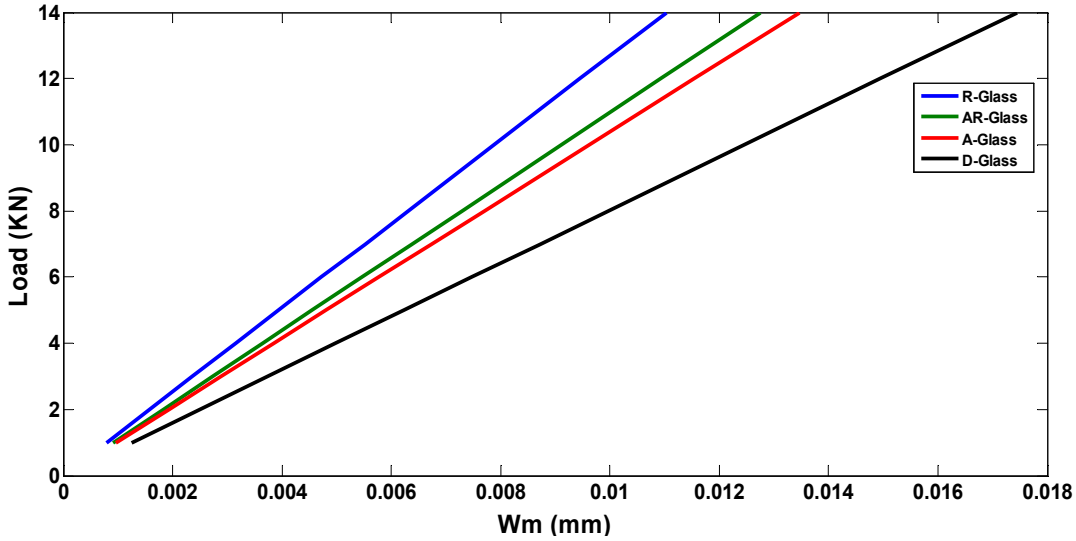

Figure (10): Effect of load on deflection of the different types of (R-glass, AR-glass, A-glass, D-glass) fiber hybrid with Aluminum 5052 honeycomb core.

QALAAI ZANISTSCIENTIFIC JOURNAL
A Scientific Quarterly Refereed Journal Issued by Lebanese French University – Erbil, Kurdistan, Iraq
Vol. (9), No (1), Spring2024
ISSN 2518-6566 (Online) - ISSN 2518-6558 (Print)

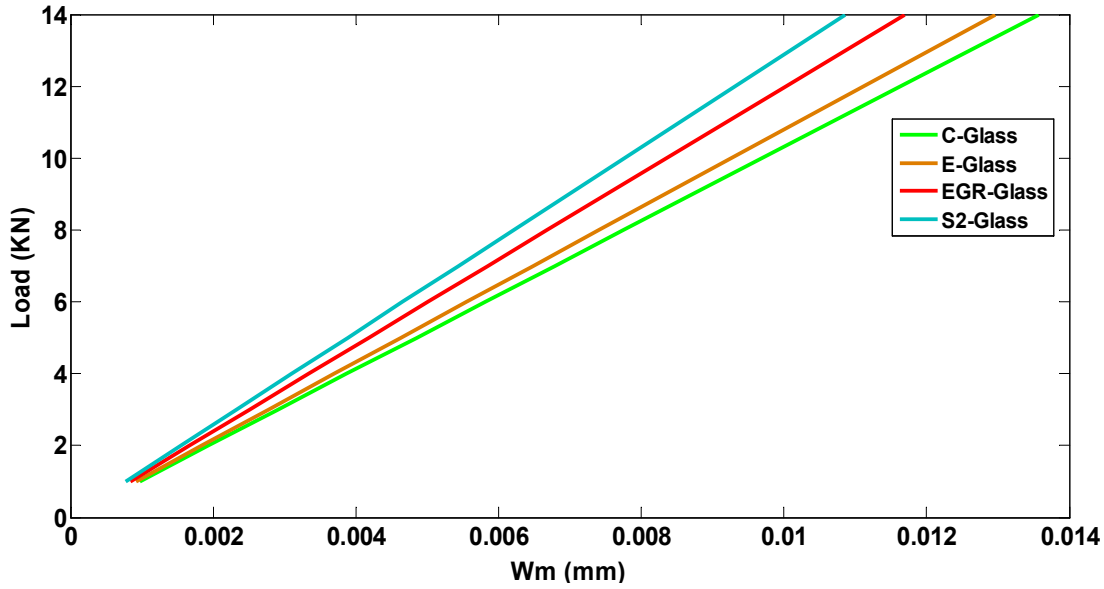

Figure (11): Effect of load on deflection of different types of (C-glass, E-glass, EGR glass, S2) fiber hybrid with Aluminum 5052 honeycomb core.

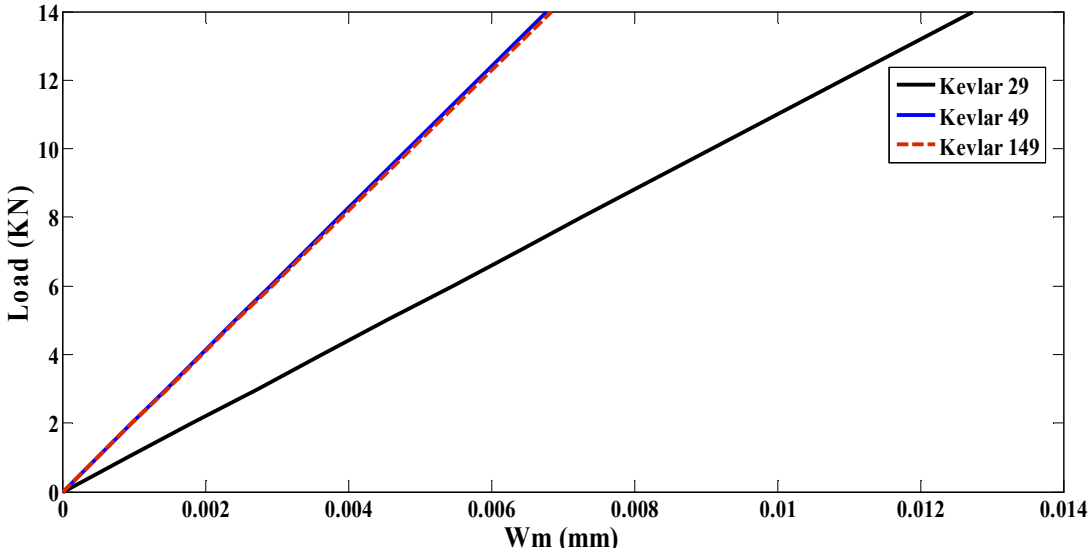

Figure (12): Effect of load on deflection of different types of Kevlar fiber hybrid with Aluminum 5052 honeycomb core.

QALAAI ZANISTSCIENTIFIC JOURNAL
A Scientific Quarterly Refereed Journal Issued by Lebanese French University – Erbil, Kurdistan, Iraq
Vol. (9), No (1), Spring2024
ISSN 2518-6566 (Online) - ISSN 2518-6558 (Print)

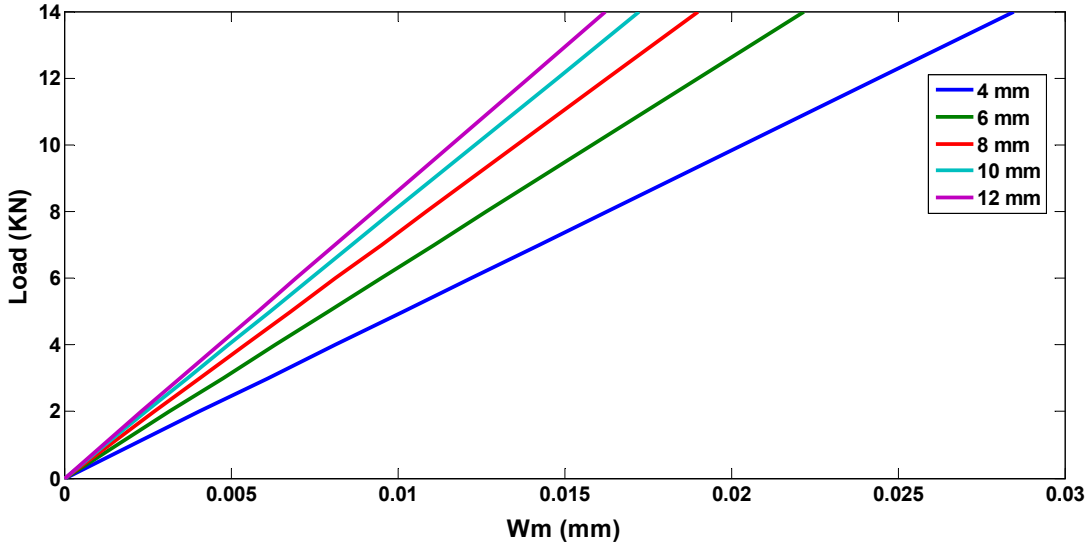

Figure (13): Effect of load on deflection of different layer thickness of E-glass fiber hybrid with Aluminum 5052 honeycomb core.

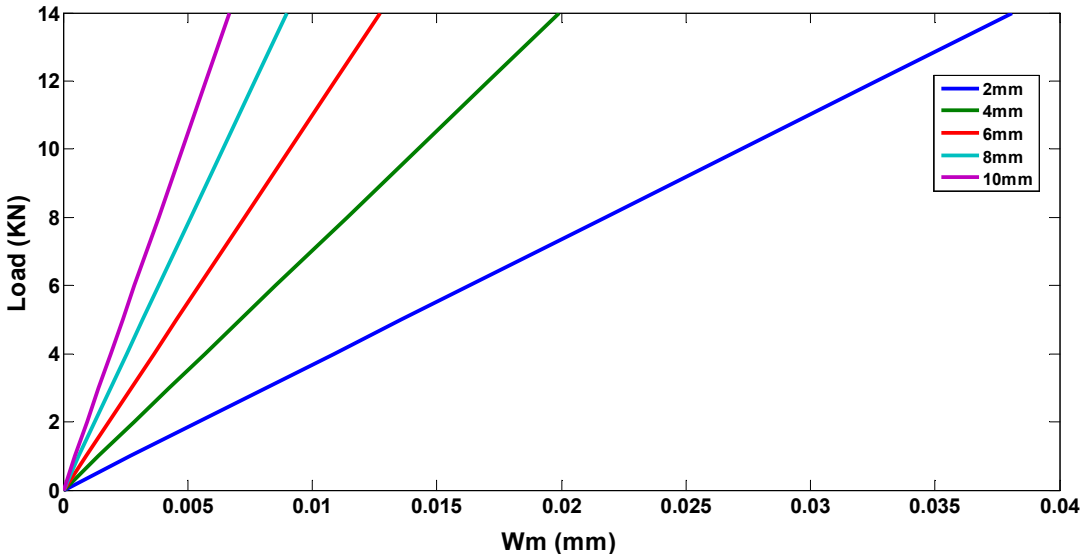

Figure (14): Effect of load on deflection of different layer thickness of Kevlar-29 fiber hybrid with Aluminum 5052 honeycomb core.

QALAAI ZANISTSCIENTIFIC JOURNAL
A Scientific Quarterly Refereed Journal Issued by Lebanese French University – Erbil, Kurdistan, Iraq
Vol. (9), No (1), Spring2024
ISSN 2518-6566 (Online) - ISSN 2518-6558 (Print)

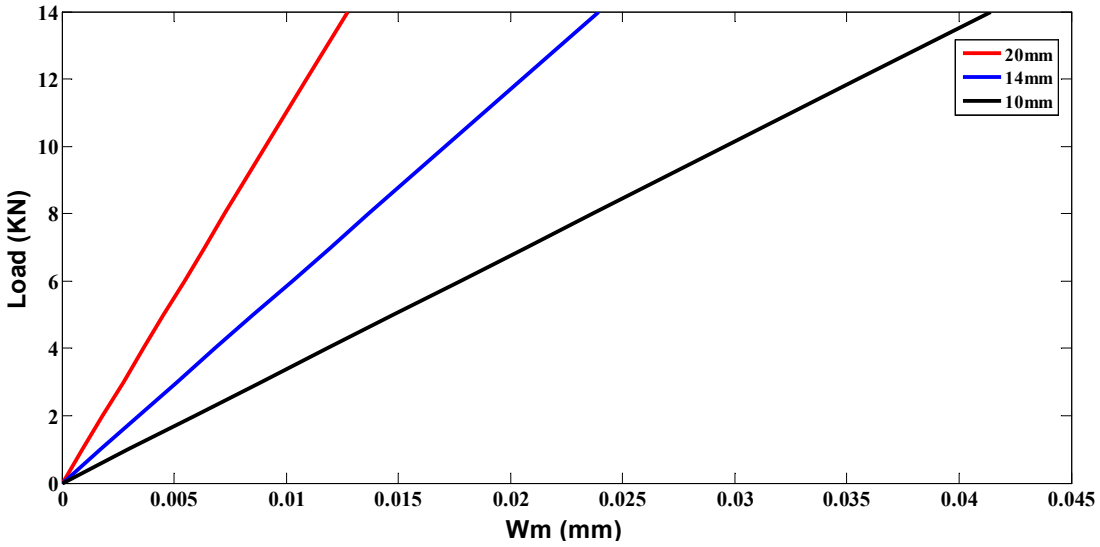

Figure (15): Effect of load on deflection of different layer thickness of Aluminum 5052 honeycomb core (20mm, 14mm, and 10mm) with Kevlar-29 fiber hybrid.

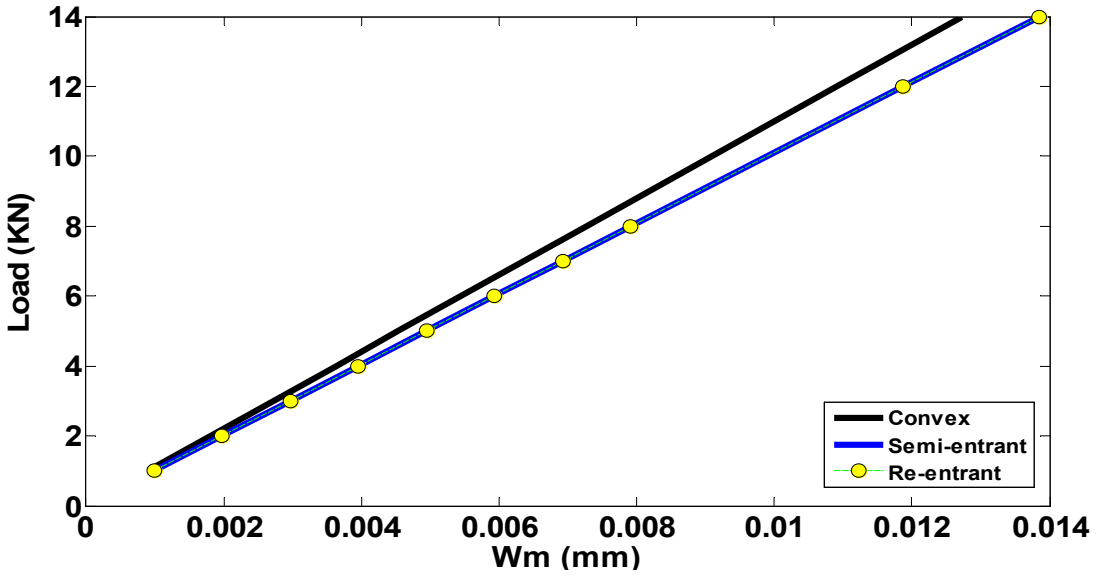

Figure (16): Effect of load on deflection of (Convex, semi-entrant, re-entrant) cell shape of Aluminum 5052 honeycomb core with Kevlar-29 fiber hybrid.

QALAAI ZANISTSCIENTIFIC JOURNAL
A Scientific Quarterly Refereed Journal Issued by Lebanese French University – Erbil, Kurdistan, Iraq
Vol. (9), No (1), Spring2024
ISSN 2518-6566 (Online) - ISSN 2518-6558 (Print)

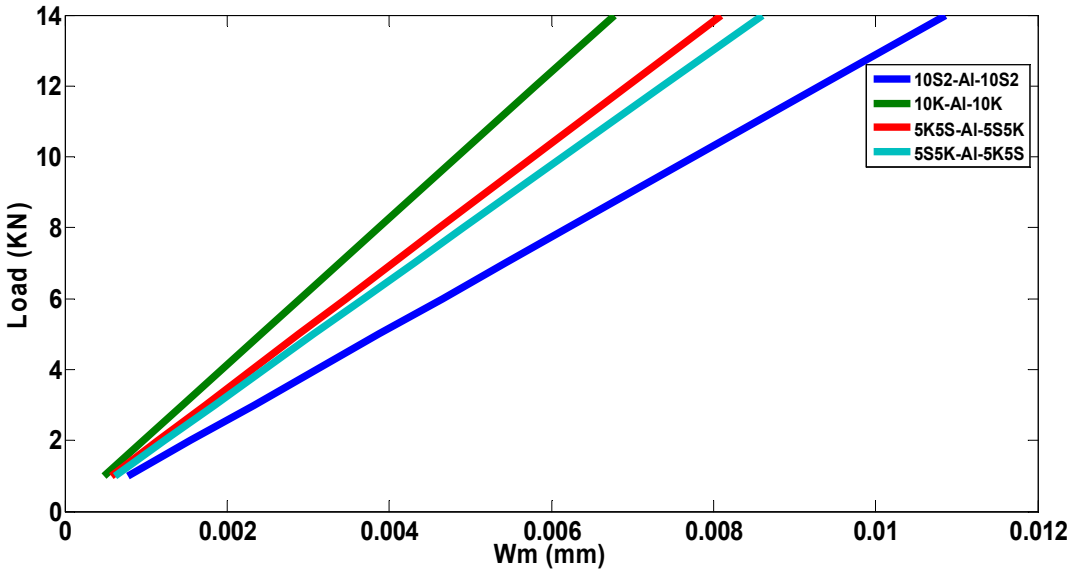

Figure (17): Effect of load on central deflection for S_2 glass fiber, Kevlar-49, and mixing layers of S_2-glass and Kevlar-49 with Al-5052 honeycomb core.

6. Conclusion

Analytical solution of multi layered symmetric laminated sandwich composite plate is a need as a first step design of new body armors. As exact solutions for calculation of the plate's maximum bending deflection is not available, the approximate solution by using Ritz method is an efficient method for solving this problem. Validated results by FE method through (ANSYS 2021R1/LS-DYNA) showed fantastic agreement with analytically modeled results. According to this validation, the ANSYS steps are correct for all cases. Through parametric investigations, the study concluded the following results:

- S2-glass and R-glass are the best two materials for energy absorption, and have minimum central deflection while compared to other examined types of glass fibers.

QALAAI ZANISTSCIENTIFIC JOURNAL
A Scientific Quarterly Refereed Journal Issued by Lebanese French University – Erbil, Kurdistan, Iraq
Vol. (9), No (1), Spring2024
ISSN 2518-6566 (Online) - ISSN 2518-6558 (Print)

- Among three examined types of Kevlar, Kevlar-49 has more energy dissipation to absorb load, and made minimum deflection because of its higher strength and modulus of elasticity as compared to other types of Kevlar.
- Changed layers and mixed S2-glass with Kevlar-49 with constant load and thicknesses; the results showed that central deflection decreases by increase Kevlar-49 layers instead of S2-glass fiber, and Kevlar-49 layers are better when placed in the front of face-sheet and absorb more load and decrease central deflection.
- While studying laminate thickness, several different laminate thicknesses changed for E-glass face-sheet, Kevlar-29 face-sheet, and aluminum 5052 honeycomb core results showed that central deflection decreases as layer thickness increased with constant load.
- Finally, the geometric of cell shapes of honeycomb core laminated has affect in reducing the plate's central deflection. The results proved that the Convex cell of honeycomb core plays a great role in absorbing the force energy as a result reduced the plate deflection by 8% than semi-entrant and re-entrant, and Kevlar-49 is better than other types because it has a greater strength and modulus of elasticity.
- Glass fibers are materials of low ductility, but when used as layers in composite plate, the plates overall deflection was reduced, and laminated S2-glass fiber better by 14.73% with compared to Kevlar-29.

References:

1. Ahmed, J. K., Agarwal, V., Pal, P., & Srivastav, V. (2013). Static and dynamic analysis of composite laminated plate. *International Journal of Innovative Technology and Exploring Engineering, 3*(6), 56-60.
2. Al-Mezrakchi, R., Al-Ramthan, A., & Alam, S. (2020). Designing and modeling new generation of advanced hybrid composite sandwich structure armors for ballistic threats in defense applications. *AIMS Materials Science, 7*(5), 608-631.
3. Al Hilli, A. (2006). Analytical and Experimental Study of High Velocity Impact on Composite Plate. *College of Engineering of Nahrain University*.
4. Baltacıoğlu, A., Civalek, Ö., Akgöz, B., & Demir, F. (2011). Large deflection analysis of laminated composite plates resting on nonlinear elastic foundations by the method of discrete singular convolution. *International Journal of Pressure Vessels and Piping, 88*(8-9), 290-300.
5. Bhimaraddi, A. (1987). Static and transient response of rectangular plates. *Thin-Walled Structures, 5*(2), 125-143.
6. Civalek, Ö. (2005). Geometrically nonlinear dynamic analysis of doubly curved isotropic shells resting on elastic foundation by a combination of harmonic differential quadrature-finite difference methods. *International Journal of Pressure Vessels and Piping, 82*(6), 470-479.
7. Civalek, Ö. (2006). Harmonic differential quadrature-finite differences coupled approaches for geometrically nonlinear static and dynamic analysis of rectangular plates on elastic foundation. *Journal of sound and vibration, 294*(4-5), 966-980.
8. Dewangan, H. C., Katariya, P. V., & Panda, S. K. (2020). Time-dependent transverse deflection responses of the layered composite plate with concentric circular cut-out. *Materials Today: Proceedings, 33*, 4961-4965.
9. Dumir, P. (1988). Nonlinear dynamic response of isotropic thin rectangular plates on elastic foundations. *Acta mechanica, 71*(1), 233-244.
10. Dumir, P., & Bhaskar, A. (1988). Nonlinear static analysis of rectangular plates on elastic foundations by the orthogonal point collocation method. *Computer methods in applied mechanics and engineering, 67*(1), 111-124.

11. Fang, H., Shi, H., Wang, Y., Qi, Y., & Liu, W. (2016). Experimental and theoretical study of sandwich panels with steel facesheets and GFRP core. *Advances in Materials Science and Engineering, 2016*.
12. Gibson, L. J., Ashby, M. F., Schajer, G., & Robertson, C. (1982). The mechanics of two-dimensional cellular materials. *Proceedings of the Royal Society of London. A. Mathematical and Physical Sciences, 382*(1782), 25-42.
13. Greene, M. E., Horlick, J., Longhurst, D. A., Miller, L. L., O'Shea, M., Otterson, D., . . . Justice, N. I. o. (2018). The Next Revision of the NIJ Performance Standard for Ballistic Resistance of Body Armor. *Annotation*.
14. Kaw, A. K. (2005). *Mechanics of composite materials*: CRC press.
15. Khdeir, A., & Reddy, J. (1989). Exact solutions for the transient response of symmetric cross-ply laminates using a higher-order plate theory. *Composites Science and Technology, 34*(3), 205-224.
16. Luo, Y., Yuan, K., Shen, L., & Liu, J. (2021). Sandwich panel with in-plane honeycombs in different Poisson's ratio under low to medium impact loads. *Reviews on Advanced Materials Science, 60*(1), 145-157.
17. Mukasey, M., Sedgwick, J. L., & Hagy, D. (2008). Ballistic resistance of body armor, nij standard-0101.06. *US Department of Justice (www. ojp. usdoj. gov/nij), 38*.
18. Nath, Y., Prithviraju, M., & Mufti, A. (2006). Nonlinear statics and dynamics of antisymmetric composite laminated square plates supported on nonlinear elastic subgrade. *Communications in Nonlinear Science and Numerical Simulation, 11*(3), 340-354.
19. Nath, Y., & Shukla, K. (2001). Non-linear transient analysis of moderately thick laminated composite plates. *Journal of sound and vibration, 247*(3), 509-526.
20. Nath, Y., Varma, K., & Mahrenholtz, D. (1986). Nonlinear dynamic response of rectangular plates on linear elastic foundation. *Computers & structures, 24*(3), 391-399.
21. Nia, A. A., Razavi, S., & Majzoobi, G. (2008). Ballistic limit determination of aluminum honeycombs—experimental study. *Materials Science and Engineering: A, 488*(1-2), 273-280.
22. Reddy, J., & Chandrashekhara, K. (1987). Recent advances in the nonlinear analysis of laminated composite plates and shells.

23. Reddy, J., & Chao, W. (1981). Non-linear bending of thick rectangular, laminated composite plates. *International Journal of Non-linear Mechanics, 16*(3-4), 291-301.
24. Reddy, J. N. (1983). Geometrically nonlinear transient analysis of laminated composite plates. *AIAA Journal, 21*(4), 621-629.
25. Reddy, J. N. (2003). *Mechanics of laminated composite plates and shells: theory and analysis*: CRC press.
26. Shen, H.-S. (1999). Large deflection of composite laminated plates under transverse and in-plane loads and resting on elastic foundations. *Composite Structures, 45*(2), 115-123.
27. Shen, H.-S. (2000). Nonlinear analysis of composite laminated thin plates subjected to lateral pressure and thermal loading and resting on elastic foundations. *Composite Structures, 49*(2), 115-128.
28. Shukla, K., & Nath, Y. (2000). Nonlinear analysis of moderately thick laminated rectangular plates. *Journal of engineering mechanics, 126*(8), 831-838.
29. Sofiyev, A., & Schnack, E. (2003). The buckling of cross-ply laminated non-homogeneous orthotropic composite conical thin shells under a dynamic external pressure. *Acta mechanica, 162*(1), 29-40.

QALAAI ZANISTSCIENTIFIC JOURNAL
A Scientific Quarterly Refereed Journal Issued by Lebanese French University – Erbil, Kurdistan, Iraq
Vol. (9), No (1), Spring2024
ISSN 2518-6566 (Online) - ISSN 2518-6558 (Print)

لێکۆینەوەی پارامیتری بۆ کۆمپۆزایت پلیتی چین چین کراو لەکەل پلیتی ساندویچ لەشێوەی شانەی هەنگ

پـوختـه:

لەم توێژینەوەیەدا چارەسەرێکی شیکەرەوەی بۆ پلیتی کامپۆزیتی کە پێکهاتووە لە چەند چینێک کە لەسەر یەکتر چین چین کراون کە لە ناوەڕاستی پلیتی کامپۆزیتەکەدا پلیتی ئەلەمنیۆمی لەشێوەی شانەی هەنگ بەستراوە بە دوو شێوازی جیاواز: یەکەم: کیڤلار لە شێوەی چەند پلیتیکی تەنك لەکەل پلیتی ئەلەمنیۆمی لە بەشی ناوەڕاستی وە چەند پلیتیکی تری تەنك لە کیڤلار بەستراوە، دووەم: ڕیشاڵی شووشەیی لە شێوەی چەند پلیتیکی تەنك لەکەل پلیتی ئەلەمنیۆمی لە بەشی ناوەڕاستی وە چەند پلیتیکی تری تەنك لە ڕیشاڵی شووشەیی بەستراوە. . لەلێکۆڵینەوەی تیۆری (بیردۆزی کلاسیکی) و ریکای شیکاری (Finite Element) بە بەرنامەی(ANSYS 2021 R1/LS-DYNA) بەکارهاتووە بۆ مۆدێلکردنی پلیتی کومپۆزیتی پاشان کاریگەری بەها جیاوازەکانی هێز بەکارهاتووە بۆ دۆزینەوەی زۆرترین بڕی چەمانەوەی پلیتەکە بە ڕیکای ڕیتز. ئەنجامە بڕواپێکراوەکان لەلایەن (Finite) Element هەوە ڕێکەوتنی تەواو لەگەڵ ئەنجامە مۆدێل کراوەکان نیشان دەدات. دواتر لێکۆڵینەوەکانی پارامیتری ئەنجام درا، جۆری مادەکان، ئەستووری لامینیت، و چەند ئەندازەیەک لە شێوەی شانەی هەنگوینەکە خوێندرانەوە. ئەنجامەکان سەلماندیان کە پلیتی ئەلەمنیۆمی لەشێوەی شانەی هەنگ لەجۆری (Convex) ڕۆڵێکی گەورە دەبینێت لە هەڵمژینی وزەکەدا لە ئەنجامدا کەمبوونەوەی چەمانەوەی پلیتەکە بە ڕێژەی 8٪ باشتر بوو لە (semi-entrant) و (Re-entrant)، ڕیشاڵی کیڤلار-49 لە جۆرەکانی تر باشترە. هەرچەندە ڕیشاڵی شووشەیی لاوازە بەڵام ووزەیەکی زیاتر هەڵدەمژێت کاتێک وەک چەند چینێک بەکاردێت لە شێوەی پلیتێکی کۆمپۆزیتی دا،بۆ نموومە ڕیشاڵی شووشەیی لە جۆری فایبەری-S_2 بە ڕێژەی 14.73 ٪ باشترە لە کیڤلار-29.

QALAAI ZANISTSCIENTIFIC JOURNAL
A Scientific Quarterly Refereed Journal Issued by Lebanese French University – Erbil, Kurdistan, Iraq
Vol. (9), No (1), Spring2024
ISSN 2518-6566 (Online) - ISSN 2518-6558 (Print)

تحقيقات بارامترية على ألواح المركبة المغلفة بالبليت ساندويجى على شكل زنزانة النحل

الملخص:
في هذا البحث استخدم التحليل النظري للوحة المتعدد الطبقات لصناعة صفائح مركبة بنوعين مختلفين: أولاً: رُكبَت (الياف كِفلر) فى شكل متعدد الطبقات مع البليت الالمنيومي على شكل (زنزانة النحل)، و كيفية تركيبه هي: مركبة من ثلاث طبقات: الطبقة الأولى هي طبقة كِفلر و الطبقة الثانية هي طبقة الأمنيومي الموضوعة عليها، و الطبقة الثالثة هي طبقة كِفلر، و الأياف الزجاجي مركبة بنفس الشكل لكن يختلف مع الأول في طبقته الأولى و الثالثة، يعني في طبقته الأولى الأياف الزجاجي و في طبقة الوسطى الأمنيوم، ثم طبقة الثالثة هي طبقة الياف الزجاجي أيضا. و في هذه العملية استخدمت النظرية الكلاسيكية للبليت المركبة من صفائح متعددة، و استخدم طريقة (ريتز) لتحديد أكثر مقدار الانحناء في الوسط البليت ثم قورن النتائج بنتيجة جيدة مع البرنامج التحليلية (Finite Element) باسم (ANSYS 2021 R1/LS-DYNA) . و اختبر فيها كل من: التغيير في نوع المواد المستعملة فيها و سمك الطبقات و في شكل بعض الخلايا من زنزانة النحل. و النتائج سَلَّمَت أَنَّ (Convex) التي في زنزانة النحل لها دور كبير في امتصاص القوة، و في النتيجة يظهر أن (Convex) قللة انحناء البليت بنسبة (8%) بالمقارنة ب (semi-entrant) و (Re-entrant)، و ظهر أن كِفلر (49) هو أفضل الأنواع بالمقارنة بأنواعه الأخرى، و الأياف الزجاجي من نوع (S_2) الذي على شكل ساندويج البليت قلل انحناء البليت الألمنيومي بنسبة (14.73%) إذا قورن ب (كِفلر 29) إذا كان له نفس خاصية البليت الألمنيومي.